



Vibration analysis of a rotating cantilever double-tapered AFGM nanobeam

Mohammadali Ghafarian¹ · Bijan Shirinzadeh¹ · Weichen Wei¹

Received: 15 February 2020 / Accepted: 30 March 2020 / Published online: 15 April 2020
© Springer-Verlag GmbH Germany, part of Springer Nature 2020

Abstract

Nano-structures such as carbon nanotube, nanobeams, nanorods, nanoplates, nanowires, and nanorings are tremendously used in various small-scale devices and investigating their dynamical behavior has been a hot research topic and can be beneficial in manufacturing and designing new devices. Therefore, free vibration analysis of a rotating cantilever double-tapered axially functionally graded material nanobeam is presented in this work. Due to the nano-scale dimension, classical beam theories are incompetent at describing the behavior of nanobeams. Thus, the nonlocal Eringen elasticity theory is adopted which considers the nonlocal scale effect for the small dimension effect of the structure of a nano-scale mechanism. The proposed nanobeam structure is assumed to taper linearly in two different axes, and its material is changing nonlinearly along its length. The equation of motion of the proposed system is found utilizing the nonlocal Eringen theory, and it is solved using a semi-analytical technique, differential transform method. Mode shapes and natural frequencies are extracted as the solution of the equation of motion of the system. Furthermore, the effects of several parameters such as nonlocal scale effect, rotational speed, hub radius, and taper ratios on the natural frequencies are investigated. Finally, a comparison between the presented work and other reported results show an excellent agreement.

1 Introduction

Beams are crucial components in any mechanical structure such as automotive and aircraft components, machine frames, and other mechanical or structural systems that contain beam structures and are designed to carry structural loads. Flexure beams with small thickness have been used widely in micro/nano manipulation mechanisms and grippers. Many studies (Ghafarian et al. 2018, 2019; Zhang et al. 2017; Pinskiier and Shirinzadeh 2019; Gu et al. 2018) have been conducted on the design, analysis, and optimization of flexure beams for Micro/Nano electromechanical systems' (MEMS/NEMS) applications. Dynamic analysis of micro/nano beams is essential as the strength and desired performances of the structure directly related to the dynamic characteristics. Therefore, during the past decade, there have been important insights into the modeling of the vibrational behavior of such micro/nano

structures. Nanobeams are an essential component which have been used in biomedical sensors (e-nose), atomic force microscopy (AFM), nanoscale memory devices, photonic crystal nanobeam cavities, resonant Lorentz force magnetic field sensors, and NEMS. CNTs, nanorods, nanoplates, nanowires, nanorings, graphenes and microtubules can also be formulated like a nanobeam. Classical beam theories such as Euler–Bernoulli theory, Rayleigh theory, Timoshenko theory (Ghafarian and Ariaei 2016a, 2019), Reddy theory, and Levinson theory are inappropriate for modeling of small scale effect on nanobeams. Therefore, many size-dependent continuum theories have been established for describing the mechanical behavior of micro/nano scale mechanisms and structures. Among these theories, nonlocal elasticity theory by Eringen (1972, 1983) has been widely used and adopted to explain the behavior of those minuscule mechanical systems (Ghafarian and Ariaei 2016b; Moutlana and Adali 2019; Yayli 2014; Santos and Soares 2012; Wang 2017; Eptaimeros et al. 2020; Jha and Dasgupta 2019). Aranda-Ruiz et al. (2012) calculated the natural frequencies of the flapwise bending vibrations of a non-uniform rotating nano cantilever, considering the true spatial variation of the axial force due to the rotation. The nanobeam's height was

✉ Mohammadali Ghafarian
Mohammadali.Ghafarian@monash.edu

¹ Robotics and Mechatronics Research Laboratory (RMRL),
Department of Mechanical and Aerospace Engineering,
Monash University, Melbourne, VIC 3800, Australia

assumed to taper linearly along its length. The problem was formulated using the nonlocal Eringen elasticity theory and it was solved by a pseudospectral collocation method based on Chebyshev polynomials. Aydogdu (2014) studied the axial vibration of double-walled carbon nanotubes (DWCNTs) using nonlocal elasticity theory considering the van der Waals forces in the axial direction. Duan et al. (2007) calibrated the small scaling parameter of the nonlocal Timoshenko beam theory for the free vibration problem of single-walled carbon nanotubes (SWCNTs). The calibration exercise was performed by using vibration frequencies generated from MD simulations at room temperature.

On the other hand, FGMs are regarded as one of the most promising candidates for future advanced composites in many engineering sectors. These materials are deemed to have an advantageous behavior over laminated composites due to the continuous variation of their material properties yet in all three dimensions, which alleviate delamination, de-bonding, and matrix cracking initiation issues. Therefore, the mechanical problems associated with the structures constructed from FGMs have gained a huge deal of attention during recent years (Zhang et al. 2019; Rajasekaran 2013; Aubad et al. 2019; Rastehkenari 2019; Gholipour and Ghayesh 2020). Shahba et al. (2013) studied free vibration analysis of rotating tapered beams made of FGMs using a finite element approach. Karamanli (2018) investigated the free vibration behavior of two-directional FG beams subjected to various sets of boundary conditions by employing a third-order shear deformation theory. The material properties of the beam were assumed to vary exponentially in both directions. Ruocco et al. (2018) presented the buckling and free vibration analyses of nonlocal axially functionally graded Euler nanobeams based on the Hencky bar chain (HBC) model. Gorgani et al. (2019) studied the pull-in behavior of cantilever micro/nano beams made of FGMs with small-scale effects under electrostatic force. The Rayleigh–Ritz method was implemented to approximate analytical solutions for the pull-in voltage and pull-in displacement of the microbeams.

Analytical and semi-analytical solutions of the partial differential equations applied in describing engineering problems are often difficult to obtain. Thus, researchers have used different techniques to solve the differential equations in engineering problems. Some of these applied methods are differential quadrature method (DQM), generalized differential quadrature method (GDQM), homotopy perturbation method (HPM), homotopy analysis method (HAM), optimal homotopy asymptotic method (OHAM), Adomian decomposition method (ADM), finite element method (FEM), and differential transformation method (DTM) which have been used by numerous

scholars to solve the governing differential equations describing the behavior of mechanical problems. Each of the mentioned methods has its own advantages over the other methods (Ghafarian and Ariaei 2016a, b, 2019; Ragb et al. 2019; Shishesaz et al. 2019; Noghrehabadi et al. 2012; Aria and Friswell 2019). However, the analytical and semi-analytical solution methods are preferred because of the sense in the physics of the problem and convenience in parametric studies Ghafarian and Ariaei (2016a). DTM is an authentic, effective and precise technique with the ability of simple formulation and implementation and with a low computational cost. DTM employs the polynomial form to estimate the exact solution based on the Taylor series expansion. Throughout this technique, the derived differential equations of motions of the mechanical system as well as the boundary conditions are transformed into algebraic equations. Accordingly, the accurate and reliable results can be obtained throughout solving the resultant algebraic equations, without requiring computational operations. On the whole, the simplicity and high precision are the most distinguished aspects of DTM (Ghafarian and Ariaei 2016a, b, 2019; Semnani et al. 2013; Godara and Joglekar 2017).

As it was discussed in the literature review, so far some research related to the vibration characteristics of the rotating nanobeams made from different materials has been done by the researchers using various theories. However, according to the best knowledge of authors, there is no comprehensive investigation on the vibration characteristics of rotating double-tapered AFGM nanobeams considering two different taper ratios in the formulation and considering a uniform nonlinear distribution of materials throughout the structure. Therefore, in this paper, this issue is investigated to fill the detected gap in the open literature related to the mechanical vibration of rotating nanobeams. It is worth pointing out that AFGM and variable section properties of the considered rotating nanobeam leads to a partial differential equation with variable coefficients. For solving such equation, the DTM is employed as a semi-analytical approach due to reliability, accuracy, and simplicity of implementation.

Herewith, the governing differential equation alongside the boundary conditions describing the dynamic behavior of a rotating double-tapered AFGM nanobeam is derived by adapting the Euler–Bernoulli beam model of nonlocal Eringen elasticity theory. Subsequently, the separation of variables is applied to the equation that yields an equation containing the frequency of the system. Thereafter, dimensionless parameters are defined to obtain the dimensionless form of the governing equation as well as the related boundary conditions. The algebraic equations obtained by means of the transformation rules lead to a characteristic equation which should be solved numerically

to gain the dimensionless frequencies. To evaluate the performance of the semi-analytical method, verification and convergence study is adapted. The results show that the presented methodology proves to be accurate. Finally, some detailed numerical results are represented in which the first four dimensionless frequencies and the corresponding mode shapes are investigated. Consequently, the effects of various involved parameters including nonlocal scaling parameter, taper ratios, angular velocity, and hub radius are explored comprehensively. Some important results are revealed which may be useful for efficient designing of the nano-structures benefiting from rotating nanobeams such as nanosensors, biosensors, nano actuators, and other NEMS devices.

2 Nonlocal elasticity theory

Eringen nonlocal elasticity theory has been widely used for modeling of vibration of a nanobeam. Unlike the classic beam theory, a size-dependent term is considered in this theory which makes it compatible to predict vibration of a nano-scale beam. The following nonlocal constitutive stress–strain equation was proposed by Eringen (1983);

$$\left[1 - (e_0 a)^2 \nabla^2\right] \sigma_{ij} = C_{ijkl} \varepsilon_{kl} \tag{1}$$

where σ_{ij} , C_{ijkl} and ε_{kl} are the nonlocal stress, classical strain, and fourth-order elasticity tensors, respectively. e_0 is a constant determined independently for each material. a is an internal characteristic length (distance between atoms, lattice parameter, size of grain, granular distance, or distance between the C–C bonds, etc.). The parameter e_0 is estimated that the nonlocal elasticity model predicts satisfactorily the atomic dispersion curves of plane waves compared to that obtained from the atomistic lattice dynamics.

A method of identifying the small scaling parameter e_0 in the nonlocal theory is not known yet. As defined by Eringen (1983), e_0 is a constant specific to each material. Eringen proposed $e_0 = 0.39$ by matching the dispersion curves via the nonlocal theory for plane wave and Born–von Karman model of lattice dynamics at the end of the Brillouin zone. On the other hand, Eringen (1972), in his study, proposed $e_0 = 0.31$ for Rayleigh surface wave through nonlocal continuum mechanics and lattice dynamics. In general, different values for e_0 have been presented for different types of problems based on the matching of the results obtained with MD simulations to those obtained with the nonlocal continuum mechanics. Araujo dos Santos and Mota Soares (2012) studied the vibration of a SWCNT and found that the values of e_0 vary with the number of natural frequency and the SWCNT

length and diameter. Furthermore, Duan et al. (2007) claimed that instead of a constant value, the calibrated e_0 values vary with respect to length-to-diameter ratios, mode shapes, and boundary conditions of the SWCNTs.

3 Nonlocal equations of motion of a rotating double-tapered AFGM nanobeam

3.1 Material properties

In this study, it was assumed that the material properties of the nanobeam such as Young’s Modulus E and mass density ρ vary continuously according to power law form. Therefore, the material properties were considered to vary through the nanobeam axis and the material characteristics can also be assumed to vary based on power law distribution, and thus can be described using the following formulas;

$$E(x) = E_L + (E_R - E_L) \left(\frac{x}{L}\right)^n \tag{2}$$

$$\rho(x) = \rho_L + (\rho_R - \rho_L) \left(\frac{x}{L}\right)^n \tag{3}$$

where subscripts L and R are the corresponding material properties of the left and the right side of the nanobeam, respectively, and n is the non-negative power law exponent which dictates the material variation profile through the axis of the nanobeam. Table 1 shows the materials which were used for describing the nanobeam. To have a uniform distribution of both material, $n=2$ is chosen as the exponent.

3.2 Equation of motion

Nanotubes are central components to new rotating devices such as miniature motors. The rotating CNT can be represented as a cantilevered nanobeam which is assumed to be slender and satisfied Euler–Bernoulli beam theory. In this section, the nonlocal equation of motion is obtained based on the Euler–Bernoulli beam deformation theory for one rotating double-tapered AFGM nanobeam.

Figure 1 shows a nanobeam of length L which is fixed to a rigid molecular hub. The molecular hub has radius R and rotates in a counter-clockwise direction at a constant rotational speed, Ω . The nanobeam tapers through its breadth and height by the coefficients of c_b and c_h , respectively. Further, the material properties of the nanobeam change through its length.

Based on the Euler–Bernoulli beam theory, the axial and transverse displacement fields are represented as;

Table 1 Material properties of an AFGM nanobeam

| Material | Young’s modulus (E) (Gpa) | Density (ρ) ($\frac{\text{kg}}{\text{m}^3}$) |
|-----------------------------------|-------------------------------|---|
| Left: Zirconia (ZrO_2) | 200 | 5700 |
| Right: Aluminium (Al) | 70 | 2702 |

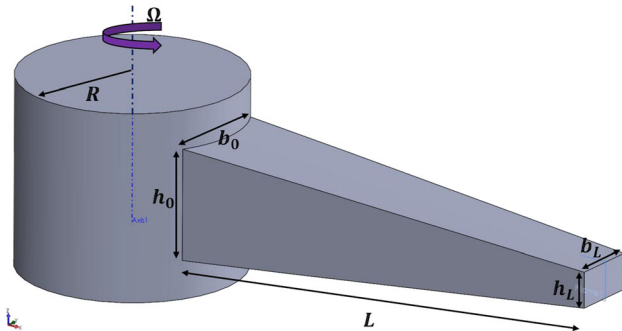


Fig. 1 Configuration of a rotating double-tapered nanobeam

$$u(x, y, z, t) = -z \frac{\partial w(x, t)}{\partial x} \tag{4}$$

$$w(x, y, z, t) = w(x, t) \tag{5}$$

where w is the transverse displacement of the neutral axis of the nanobeam. It is noteworthy that, based on some studies in the literature which considered longitudinal displacement as an independent variable for linear vibration (Lin and Wu 2005; Lin and Ro 2003), no effect was observed on the results obtained for other displacements. Considering Eqs. (4) and (5), the only non-zero strain term of the Euler–Bernoulli beam theory is described by;

$$\varepsilon_{xx} = \frac{\partial u}{\partial x} = -z \frac{\partial^2 w}{\partial x^2} \tag{6}$$

The equation of motion of a rotating nanobeam based on the Euler–Bernoulli beam theory is presented as;

$$\frac{\partial V}{\partial x} + q + \frac{\partial}{\partial x} \left(T(x) \frac{\partial w}{\partial x} \right) = \rho A \frac{\partial^2 w}{\partial t^2} \tag{7}$$

where;

$$V = \frac{\partial M}{\partial x} \tag{8}$$

$$M = \int_A z \sigma_{xx} dA \tag{9}$$

where V is the shear force, q is the external force per unit of length, $T(x)$ is the axial force due to centrifugal acceleration, r is the mass density, A is the nanobeam cross-sectional area, M is the bending moment, and σ_{xx} is the axial stress on the yz -section in the direction of x .

By considering Eqs. (1) and (6), it can be found that only one equation exists to describe the stress–strain behavior of the nanobeam;

$$\sigma_{xx} - (e_0 a)^2 \frac{\partial^2 \sigma_{xx}}{\partial x^2} = E \varepsilon_{xx} \tag{10}$$

By performing surface integration of $\int_A z(\cdot) dA$ from both sides of Eq. (10), and noting that the moment of inertia of the nanobeam cross-section is $I_y = \int_A z^2 dA$, the following equation was derived;

$$M - (e_0 a)^2 \frac{\partial^2 M}{\partial x^2} = -EI_y \frac{\partial^2 w}{\partial x^2} \tag{11}$$

By differentiating Eq. (8) with respect to x and substituting into Eq. (7), finding the term $\frac{\partial^2 M}{\partial x^2}$, and substituting it into Eq. (11), Eq. (12) was resulted as follows;

$$M = -EI_y \frac{\partial^2 w}{\partial x^2} + (e_0 a)^2 \left[\rho A \frac{\partial^2 w}{\partial t^2} - \frac{\partial}{\partial x} \left(T \frac{\partial w}{\partial x} \right) - q \right] \tag{12}$$

Now, by having the moment of inertia and using Eq. (8), the shear force of the nanobeam was derived;

$$V = -\frac{\partial}{\partial x} \left(EI_y \frac{\partial^2 w}{\partial x^2} \right) + (e_0 a)^2 \frac{\partial}{\partial x} \left[\rho A \frac{\partial^2 w}{\partial t^2} - \frac{\partial}{\partial x} \left(T \frac{\partial w}{\partial x} \right) - q \right] \tag{13}$$

Using the shear force, Eq. (13), and substituting it back into the Euler–Bernoulli equation of motion of a rotating nanobeam, Eq. (7), the final version of the equation of motion of a rotating nanobeam was obtained as;

$$\begin{aligned} & \rho A \frac{\partial^2 w}{\partial t^2} + \frac{\partial^2}{\partial x^2} \left(EI_y \frac{\partial^2 w}{\partial x^2} \right) - \frac{\partial}{\partial x} \left(T \frac{\partial w}{\partial x} \right) \\ & - (e_0 a)^2 \frac{\partial^2}{\partial x^2} \left\{ \rho A \frac{\partial^2 w}{\partial t^2} - \frac{\partial}{\partial x} \left(T \frac{\partial w}{\partial x} \right) \right\} \\ & = q - (e_0 a)^2 \frac{\partial^2 q}{\partial x^2} \end{aligned} \tag{14}$$

As the nanobeam tapers linearly from its breadth and height, the following assumptions were made;

$$c_b = 1 - \frac{b_L}{b_0} \tag{15}$$

$$c_h = 1 - \frac{h_L}{h_0} \tag{16}$$

$$A = A_0(1 - c_b \frac{x}{L})(1 - c_h \frac{x}{L}) \tag{17}$$

$$I_y = I_{y_0}(1 - c_b \frac{x}{L})(1 - c_h \frac{x}{L})^3 \tag{18}$$

where c_b and c_h should be considered lower than 1 to avoid having zero nanobeam’s height and breadth between its ends.

According to Ghafarian and Ariaei (2016a, b), the centrifugal force $T(x)$ at a distance x from the clamped end of nanobeam can be expressed as follows;

$$T(x) = \int_x^L \rho A \Omega^2 (R + \Lambda) d\Lambda \\ = A_1(L - x) + A_2(L^2 - x^2) + A_3(L^3 - x^3) \\ + A_4(L^4 - x^4) + A_5(L^5 - x^5) + A_6(L^6 - x^6) \tag{19}$$

where A_i ($i = 1, \dots, 6$) are constants and were formulated and presented in “Appendix A”. Substituting the FGM formulations, Eqs. (2) and (3), the centrifugal force, Eq. (19), and the taper assumptions, Eqs. (15)–(18), into the Eq. (14), the equation of motion of a rotating Euler–Bernoulli double-tapered AFGM nanobeam was obtained as follows;

$$B_1 \frac{\partial^2 w}{\partial t^2} + B_2 \frac{\partial^4 w}{\partial x^4} + B_3 \frac{\partial^3 w}{\partial x^3} + B_4 \frac{\partial^2 w}{\partial x^2} + B_5 \frac{\partial w}{\partial x} + B_6 \frac{\partial^3 w}{\partial x \partial t^2} \\ + B_7 \frac{\partial^4 w}{\partial x^2 \partial t^2} \\ = q - (e_0 a)^2 \frac{\partial^2 q}{\partial x^2} \tag{20}$$

B_i ($i = 1, \dots, 7$) are functions of x and were shown in “Appendix B”.

3.3 Boundary conditions

Boundary conditions of a cantilever nanobeam are described as below;

Transverse displacement and angle of bending are zero at the fixed end of nanobeam;

$$w = 0, \text{ At, } x = 0 \tag{21}$$

$$\frac{\partial w}{\partial x} = 0, \text{ At, } x = 0 \tag{22}$$

Bending moment and shear force are zero at the free end of nanobeam;

$$M = 0, \text{ At, } x = L \tag{23}$$

$$V = 0, \text{ At, } x = L \tag{24}$$

4 Free vibration analysis of the system

4.1 Free vibration analysis

In this section, free vibration analysis of a rotating double-tapered AFGM nanobeam is investigated. For this purpose, initially, the external force was neglected, and later a harmonic motion was assumed as the following form;

$$w(x, t) = u(x)e^{i\omega t} \tag{25}$$

where $u(x)$ is the amplitude functions of transverse displacement, and ω is the circular natural frequency.

4.2 Dimensionless parameters, nonlocal equation of motion, and boundary conditions

For convenience and also comparing the results with other articles, the following dimensionless parameters are introduced:

$$\bar{x} = \frac{x}{L} \\ \bar{w} = \frac{w}{L} \\ \bar{u} = \frac{u}{L} \\ \tau = \frac{e_0 a}{L} \\ \delta = \frac{R}{L} \\ \bar{E} = \frac{E_L - E_R}{E_L} \\ \bar{\rho} = \frac{\rho_L - \rho_R}{\rho_L} \\ \bar{\Omega} = \Omega \sqrt{\frac{\rho_L A_0}{E_L I_{y_0}}} L^2 \\ \bar{\omega} = \omega \sqrt{\frac{\rho_L A_0}{E_L I_{y_0}}} L^2 \tag{26}$$

where \bar{x} is the dimensionless location along the length of nanobeam, \bar{w} is the dimensionless transverse displacement, \bar{u} is the dimensionless amplitude functions of transverse displacement, τ is the dimensionless nonlocal scaling parameter, δ is the dimensionless hub radius, \bar{E} is the dimensionless Young’s modulus, $\bar{\rho}$ is the dimensionless density, $\bar{\Omega}$ is the dimensionless rotational speed, and $\bar{\omega}$ is the dimensionless natural frequency. Substituting Eq. (25) and dimensionless parameters (26) into Eqs. (20) and (21)–(24), the dimensionless form of the nonlocal equation of motion, along with the nonlocal boundary conditions were obtained, respectively, as explained in the following.

5 Dimensionless nonlocal equation of motion

The dimensionless nonlocal equation of motion was derived and shown in Eq. (27);

$$C_0\bar{u} + C_1 \frac{d\bar{u}}{d\bar{x}} + C_2 \frac{d^2\bar{u}}{d\bar{x}^2} + C_3 \frac{d^3\bar{u}}{d\bar{x}^3} + C_4 \frac{d^4\bar{u}}{d\bar{x}^4} = 0 \tag{27}$$

C_i ($i = 0, \dots, 4$) are functions of \bar{x} and were shown in “Appendix C”. Equation (27) is a linear fourth order homogenous ordinary differential equation that describes the behavior of the nanobeam system.

6 Dimensionless nonlocal boundary conditions

The dimensionless nonlocal boundary conditions were derived and shown in Eqs. (28)–(31);

Dimensionless transverse displacement at the fixed end of nanobeam;

$$\bar{u} = 0, \text{ At, } \bar{x} = 0 \tag{28}$$

Dimensionless angle of bending at the fixed end of nanobeam;

$$\frac{d\bar{u}}{d\bar{x}} = 0, \text{ At, } \bar{x} = 0 \tag{29}$$

Dimensionless nonlocal bending moment at the free end of nanobeam;

$$\bar{M} = D_2 \frac{d^2\bar{u}}{d\bar{x}^2} + D_1 \frac{d\bar{u}}{d\bar{x}} + D_0\bar{u} = 0, \text{ At, } \bar{x} = 1 \tag{30}$$

Dimensionless nonlocal shear force at the free end of nanobeam;

$$\bar{V} = E_3 \frac{d^3\bar{u}}{d\bar{x}^3} + E_2 \frac{d^2\bar{u}}{d\bar{x}^2} + E_1 \frac{d\bar{u}}{d\bar{x}} + E_0\bar{u} = 0, \text{ At, } \bar{x} = 1 \tag{31}$$

D_i ($i = 0, 1, 2$) and E_i ($i = 0, 1, 2, 3$) are functions of \bar{x} and were shown in “Appendices D” and “E”.

6.1 Differential transform method (DTM)

DTM is a beneficial and appropriate semi-analytical method for finding the solution of a differential equation. Generally, this technique consists of two differential and inverse differential transformations. If function $\bar{u}(\bar{x})$ is analytic in domain D , and $\bar{x} = \bar{x}_0$ represents any point in this domain, the differential transformation of the function $\bar{u}(\bar{x})$ is then presented by;

$$U(m) = \frac{1}{m!} \left[\frac{d^m \bar{u}(\bar{x})}{d\bar{x}^m} \right] \Big|_{\bar{x}=\bar{x}_0} \tag{32}$$

where, $\bar{u}(\bar{x})$ is the original function and $U(m)$ is the m^{th} order differential transformation of $\bar{u}(\bar{x})$.

On the other hand, the inverse differential transformation of $U(m)$ is also defined as;

$$\bar{u}(\bar{x}) = \sum_{m=0}^{\infty} U(m)(\bar{x} - \bar{x}_0)^m \tag{33}$$

In practical applications, the function $\bar{u}(\bar{x})$ is expressed by a finite series and Eq. (33) can be rewritten as follows;

$$\bar{u}(\bar{x}) = \sum_{m=0}^s U(m)(\bar{x} - \bar{x}_0)^m \tag{34}$$

Equation (34) implies that $\bar{u}(\bar{x}) = \sum_{m=s+1}^{\infty} U(m)(\bar{x} - \bar{x}_0)^m$ is negligibly small. The number of terms, s , is chosen as the convergence of natural frequencies is satisfied. Also, \bar{x}_0 is considered as zero.

The properties that are useful in the transformation of the differential equation and the boundary conditions are tabulated in Tables 2 and 3, respectively.

By applying the DTM technique from Table 2, the nonlocal equation of motion for a rotating double-tapered AFGM nanobeam, Eq. (27), can be rewritten as follows;

$$F_1 U(m-4) + F_2 U(m-3) + F_3 U(m-2) + F_4 U(m-1) + F_5 U(m) + F_6 U(m+1) + F_7 U(m+2) + F_8 U(m+3) + F_9 U(m+4) = 0 \tag{35}$$

In addition, by implementing the DTM technique from Table 3, the nonlocal boundary conditions can also be rewritten as follows;

$$U(0) = 0, \text{ At, } \bar{x} = 0 \tag{36}$$

$$U(1) = 0, \text{ At, } \bar{x} = 0 \tag{37}$$

Table 2 DTM theorems used for the equation of motion

| Original function | Transform function |
|--|--|
| $f(\bar{x}) = g(\bar{x}) \pm h(\bar{x})$ | $F(m) = G(m) \pm H(m)$ |
| $f(\bar{x}) = \alpha g(\bar{x})$ | $F(m) = \alpha G(m)$ |
| $f(\bar{x}) = g(\bar{x})h(\bar{x})$ | $F(m) = \sum_{j=0}^m G(m-j)H(j)$ |
| $f(\bar{x}) = \frac{d^m g(\bar{x})}{d\bar{x}^m}$ | $F(m) = \frac{(m+n)!}{m!} G(m+n)$ |
| $f(\bar{x}) = \bar{x}^n$ | $F(m) = \delta(m-n) = \begin{cases} 0 & \text{if } m \neq n \\ 1 & \text{if } m = n \end{cases}$ |

Table 3 DTM theorems used for the boundary conditions

| $\bar{x} = 0$ | | $\bar{x} = 1$ | |
|----------------------------|-----------------|----------------------------|--|
| Original B.C | Transformed B.C | Original B.C | Transformed B.C |
| $f(0) = 0$ | $F(0) = 0$ | $f(1) = 0$ | $\sum_{m=0}^{\infty} F(m) = 0$ |
| $\frac{df}{dx}(0) = 0$ | $F(1) = 0$ | $\frac{df}{dx}(1) = 0$ | $\sum_{m=0}^{\infty} mF(m) = 0$ |
| $\frac{d^2f}{dx^2}(0) = 0$ | $F(2) = 0$ | $\frac{d^2f}{dx^2}(1) = 0$ | $\sum_{m=0}^{\infty} m(m-1)F(m) = 0$ |
| $\frac{d^3f}{dx^3}(0) = 0$ | $F(3) = 0$ | $\frac{d^3f}{dx^3}(1) = 0$ | $\sum_{m=0}^{\infty} m(m-1)(m-2)F(m) = 0$ |
| $\frac{d^4f}{dx^4}(0) = 0$ | $F(4) = 0$ | $\frac{d^4f}{dx^4}(1) = 0$ | $\sum_{m=0}^{\infty} m(m-1)(m-2)(m-3)F(m) = 0$ |

$$\bar{M} = \sum_{m=0}^{\infty} \{G_1m(m-1) + (e_0a)^2[G_2 + G_3m]\}U(m) = 0, \text{ At, } \bar{x} = 1 \tag{38}$$

$$\bar{V} = \sum_{m=0}^{\infty} \{H_1m(m-1)(m-2) + H_2m(m-1) + (e_0a)^2[H_3 + H_4m(m-1) + H_5m]\}U(m) = 0, \text{ At, } \bar{x} = 1 \tag{39}$$

Coefficients F_i ($i = 1, \dots, 9$), G_i ($i = 1, 2, 3$), and H_i ($i = 1, \dots, 5$) were derived and shown in “Appendices F, G”, and “H”, respectively. It is worthy of mention that the function coefficients represented in “Appendices C, D, E, F, G”, and “H” are dimensionless. \bar{M} and \bar{V} are the transformed dimensionless nonlocal bending moment and shear force at the free end of the nanobeam, respectively. Applying the nonlocal boundary conditions expressed in Eqs. (36)–(39) in Eq. (35) and considering $U(2) = C_1$ and $U(3) = C_2$, the following expression was obtained;

$$A_{i1}(\bar{\omega})C_1 + A_{i2}(\bar{\omega})C_2 = 0, i = 1, 2 \tag{40}$$

where C_1 and C_2 are constant, and $A_{i1}(\bar{\omega})$ and $A_{i2}(\bar{\omega})$ are polynomials with respect to $\bar{\omega}$. The dimensionless natural frequencies are the eigenvalues of Eq. (40) and they were calculated by solving the following determinant when equals to zero;

$$\begin{vmatrix} A_{11}(\bar{\omega}) & A_{12}(\bar{\omega}) \\ A_{21}(\bar{\omega}) & A_{22}(\bar{\omega}) \end{vmatrix} = 0 \tag{41}$$

This determinant provides a single polynomial equation for determining the dimensionless natural frequencies, $\bar{\omega}$. To determine the value of the j th natural frequency, the following convergence criterion may be used;

$$\left| \bar{\omega}_j^{(q)} - \bar{\omega}_j^{(q-1)} \right| \leq \varepsilon, \quad j = 1, 2, 3, \dots \tag{42}$$

where q is the iteration counter, $\bar{\omega}_j$ is the estimated value of the j th dimensionless natural frequency, and ε is a tolerance parameter and a sufficiently small number. After calculating the natural frequencies, the mode shapes can be obtained by deriving the following relation from Eq. (40);

$$C_2 = -\frac{A_{11}(\bar{\omega}_j)}{A_{12}(\bar{\omega}_j)}C_1 \tag{43}$$

Applying Eq. (43), $U_j(m)$ can be expressed in terms of $\bar{\omega}_j$ and C_1 as follows;

$$U_j(m) = U(\bar{\omega}_j, C_1) \tag{44}$$

Having $U_j(m)$ related to each natural frequency and implementing inverse of DTM, the mode shape related to that natural frequency was obtained by the following equation;

$$\bar{u}_j(\bar{x}) = \sum_{m=0}^s U_j(m)\bar{x}^m \tag{45}$$

7 Results and discussions

In this section, the obtained results of the mathematical modeling are presented and comparisons are made to the previous studies to prove the accuracy of modeling and results.

7.1 FGM properties

The proposed nanobeam system is made of FGM. This means that the mechanical properties of the nanobeam are dependent on the specific position in itself and are changing by position. This trend in the proposed modeling was

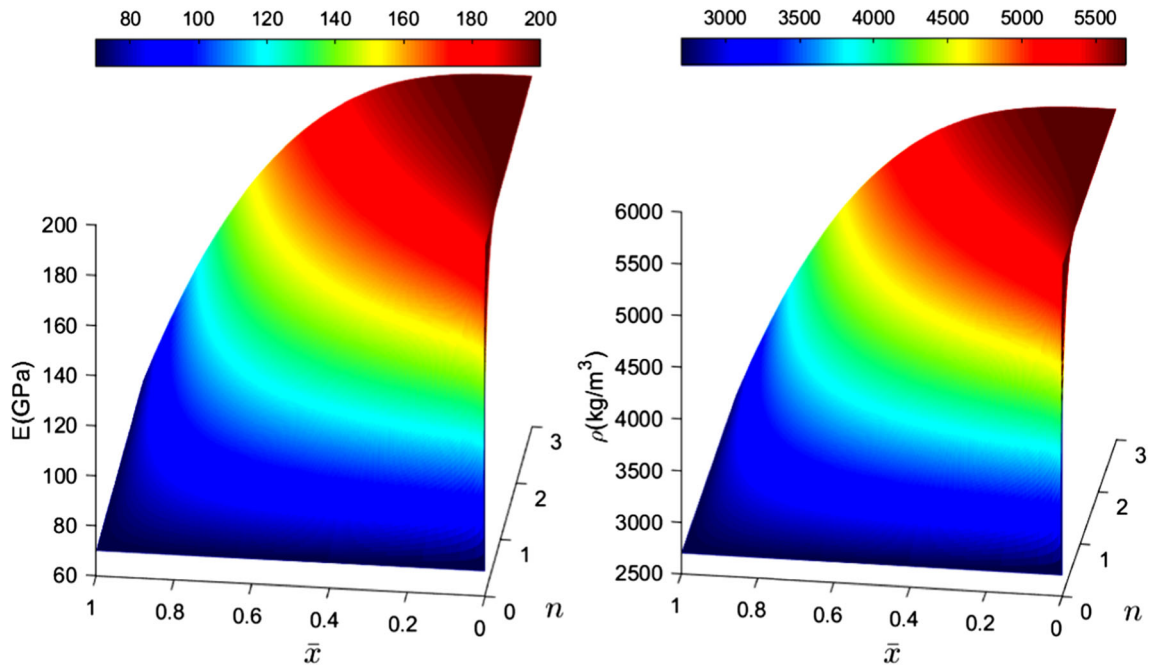


Fig. 2 Variation of Young’s modulus and mass density with respect to the exponent and dimensionless location along the length of nanobeam

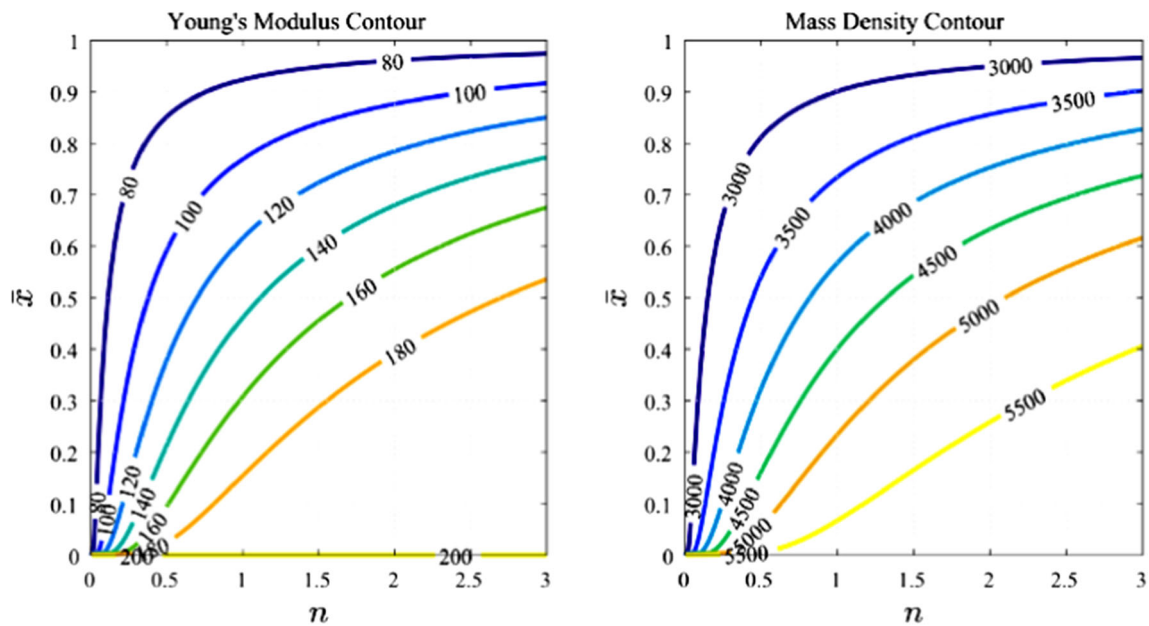


Fig. 3 The contour of Young’s modulus and mass density with respect to the exponent and dimensionless location along the length of nanobeam

formulated by Eqs. (2) and (3), which $n = 2$ was assumed. Figures 2, 3 and 4 show how the mechanical properties are changing by changing in the exponent and the position along the length of the nanobeam. Figure 2 is the 3D model of this trend with respect to \bar{x} and n . Figure 3 is the contour of this 3D model and numbers inside of the left figure show the Young’s Modulus and the numbers inside of the right figure show the mass density. It is obvious that at the very

left side of the nanobeam ($\bar{x} = 0$) the only material is Zirconia and at the very right side of the nanobeam ($\bar{x} = L$) the only material is Aluminium. Figure 4 shows the trend of changing of E and ρ along the length of the nanobeam for the exponent equals to 2. According to Fig. 4, the local Young’s modulus and mass density decrease when becoming closer to the end $x = L$. The Young’s modulus reduces faster than the mass density as getting closer to the

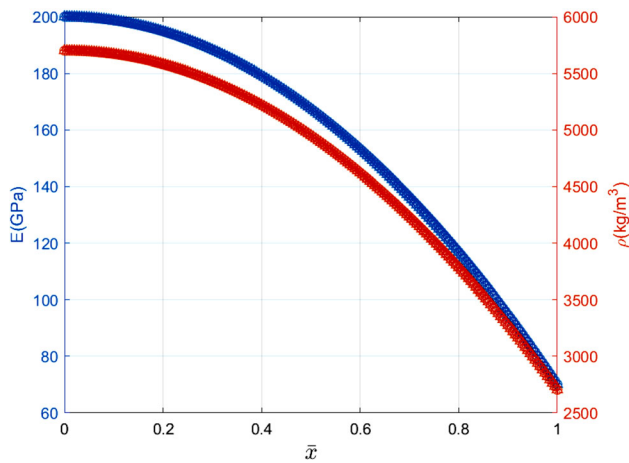


Fig. 4 Variation of Young’s modulus and mass density with respect to the dimensionless location along the length of nanobeam ($n = 2$)

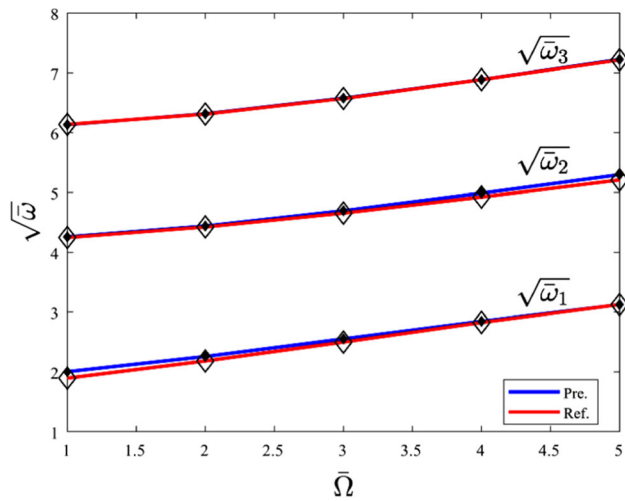


Fig. 5 Variation of dimensionless natural frequency against the dimensionless rotational speed of a rotating nanobeam, filled (Present); unfilled (Aranda-Ruiz et al. 2012)

Table 4 Geometry properties of an AFGM tapered rotating beam

| $\bar{\Omega}$ | c_b | c_h | A_0 (m ²) | I_{y_0} (m ⁴) | τ | δ | L (m) |
|----------------|-------|-------|-------------------------|-----------------------------|--------|----------|---------|
| 10.6521 | 0 | 0.6 | 0.0225 | 1.17187e−5 | 0 | 0 | 6 |

end $x = L$. Reasons for that are the dimensionless Young’s modulus reduction ($\frac{E_L - E_R}{E_L} \times 100 = 65\%$) is higher than the dimensionless density reduction ($\frac{\rho_L - \rho_R}{\rho_L} \times 100 \cong 52.6\%$).

Table 5 First five dimensionless natural frequencies of an AFGM tapered rotating beam

| Mode no. | Present | Shahba et al. (2013) |
|----------|----------|----------------------|
| 1 | 12.6432 | 12.3292 |
| 2 | 30.0557 | 29.3931 |
| 3 | 57.1080 | 57.0114 |
| 4 | 95.9109 | 97.0683 |
| 5 | 146.9954 | 150.0166 |

Table 6 Geometry properties of a rotating ZrO₂ nanobeam

| c_b | c_h | A_0 (nm ²) | I_{y_0} (nm ⁴) | τ | δ | L (nm) |
|-------|-------|--------------------------|------------------------------|--------|----------|----------|
| 0 | 0 | 8 | 8/3 | 0.2 | 1 | 250 |

Table 7 Geometry properties of an AFGM double-tapered rotating nanobeam

| $\bar{\Omega}$ | c_b | c_h | A_0 (nm ²) | I_{y_0} (nm ⁴) | τ | δ | L (nm) |
|----------------|-------|-------|--------------------------|------------------------------|--------|----------|----------|
| 3 | 0.4 | 0.4 | 8 | 8/3 | 0.1 | 0.5 | 250 |

7.2 Validation of results

For validation purposes, the results are compared with Shahba et al. (2013) and Aranda-Ruiz et al. (2012). Shahba et al. (2013) investigated the vibration analysis of an AFGM tapered rotating beam. Material and geometry properties of the analysis were chosen as shown in Tables 1 and 4, respectively. Table 5, shows the first five dimensionless natural frequencies obtained from the presented study and Shahba et al. (2013). It can be seen that good accuracy was achieved.

Investigation of a rotating nanobeam was done by Aranda-Ruiz et al. (2012) and the results are compared with the presented study. The geometry properties of the analysis were chosen as shown in Tables 6. Figure 5 shows the result of this comparison which the first three dimensionless natural frequencies were plotted against different dimensionless rotational speeds. It can be noted that the results had a good overlap and the accuracy of the modeling was guaranteed.

Fig. 6 Convergence of the first four dimensionless natural frequencies

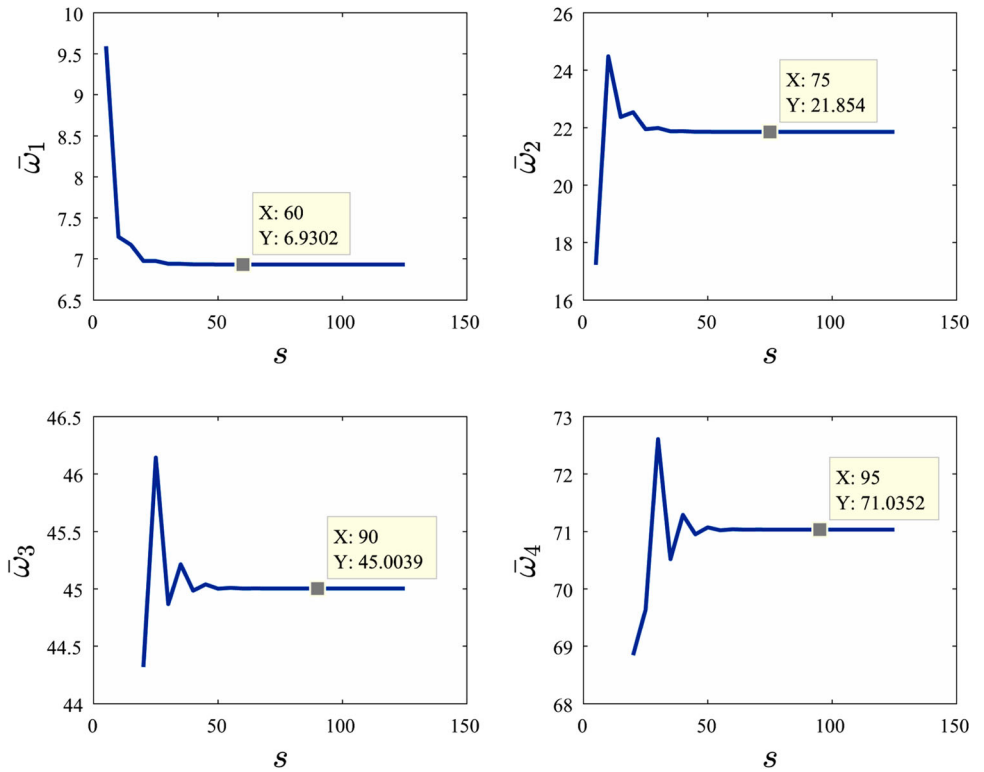


Table 8 First four natural frequencies of an AFGM double-tapered rotating nanobeam

| Mode No | Dimensionless natural frequency ($\bar{\omega}$) |
|---------|--|
| 1 | 6.9302 |
| 2 | 21.8540 |
| 3 | 45.0039 |
| 4 | 71.0352 |

7.3 Results of the presented nanobeam system and mathematical modeling

All numerical results presented in this section are based on the numerical data tabulated in Tables 1 and 7.

Slenderness Ratio (SR) is defined as the length of the nanobeam to the smallest size of the cross-section of it. The behavior of a nanobeam is closer to the nonlocal Euler–Bernoulli beam theory by a larger SR quantity due to the fact that the effects of shear deformation and rotatory inertia become negligible. In the presented work, the smallest size of the cross-section (h) is changing through the nanobeam’s length from $h_0=2$ nm to $h_l=1.2$ nm. Consequently, the SR changes from 125 to 208.3. Therefore, as a result of having large SR (meaning slender nanobeam), it can be concluded that there is no significant difference

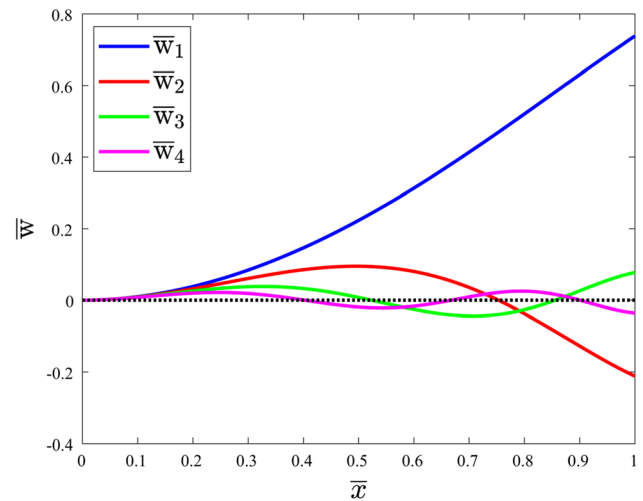


Fig. 7 Mode shapes of an AFGM double-tapered rotating nanobeam

between the vibrational frequencies of Euler–Bernoulli and Timoshenko nanobeams and the nonlocal Euler–Bernoulli beam theory can be used to describe the behavior of the considered nanobeam system (Kikidis and Papadopoulos 1992; Aydin 2013).

In Fig. 6, the convergence of the first four dimensionless natural frequencies is introduced. Here, it was necessary to take 95 terms to evaluate up to the fourth dimensionless natural frequency to four-digit precision. Therefore, the number of the terms, s , mentioned in Eq. (34) is 95 for the

Fig. 8 Effect of the dimensionless nonlocal scaling parameter on the natural frequencies of an AFGM double-tapered rotating nanobeam

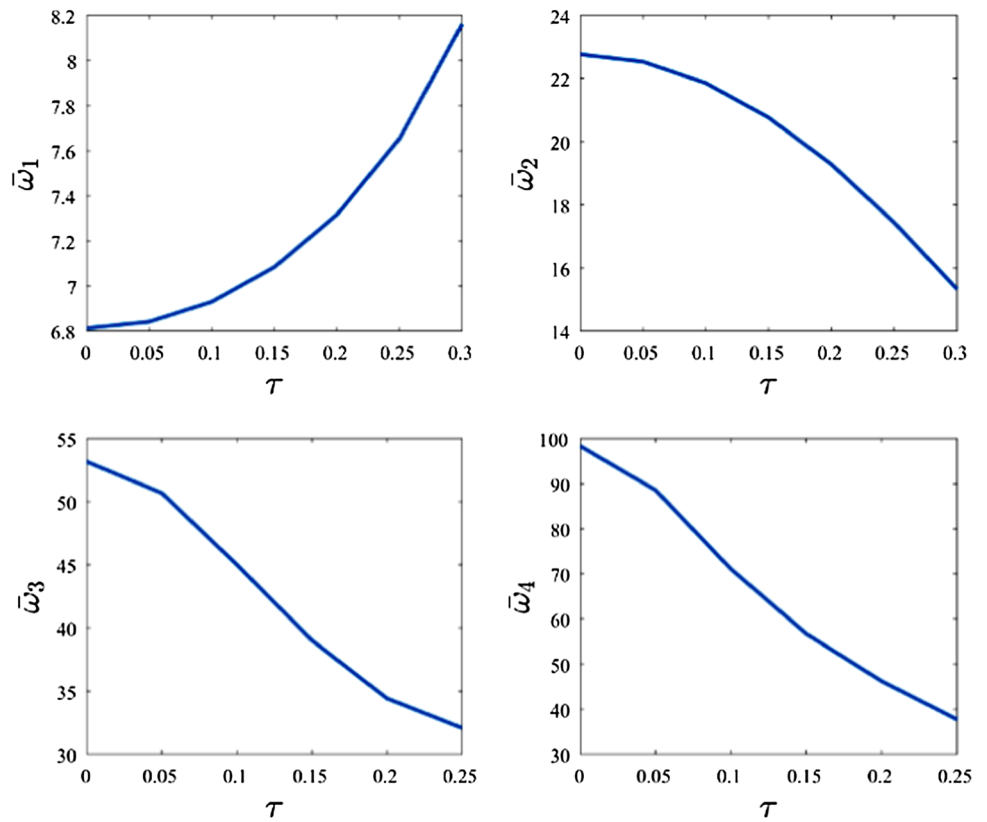
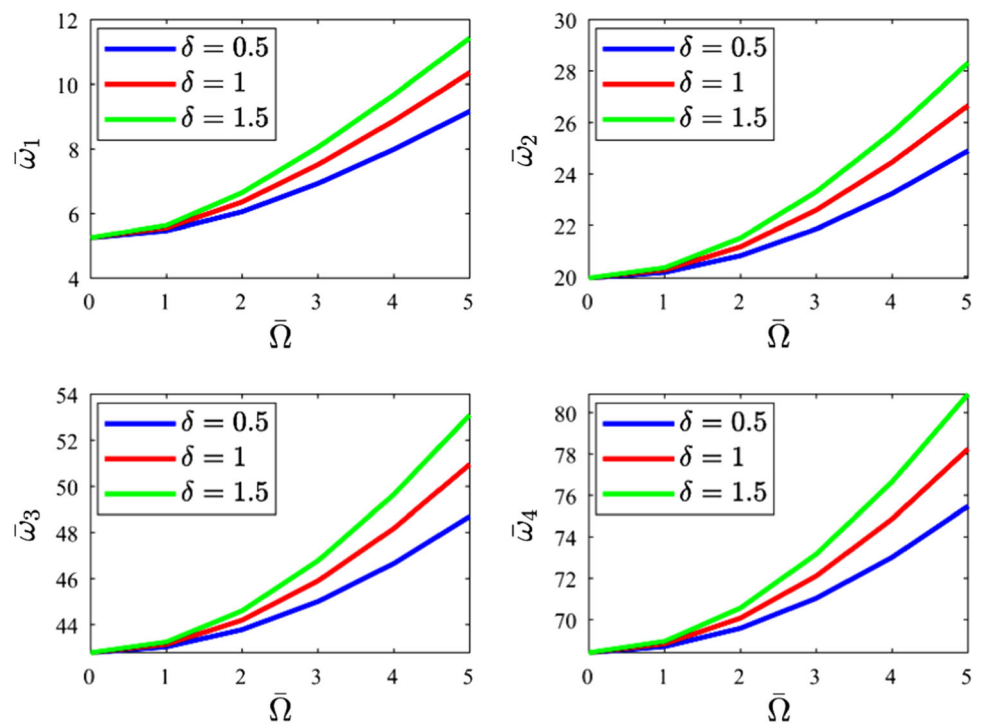


Fig. 9 Effect of rotational speed and hub radius on the natural frequencies of a rotating double-tapered AFGM nanobeam



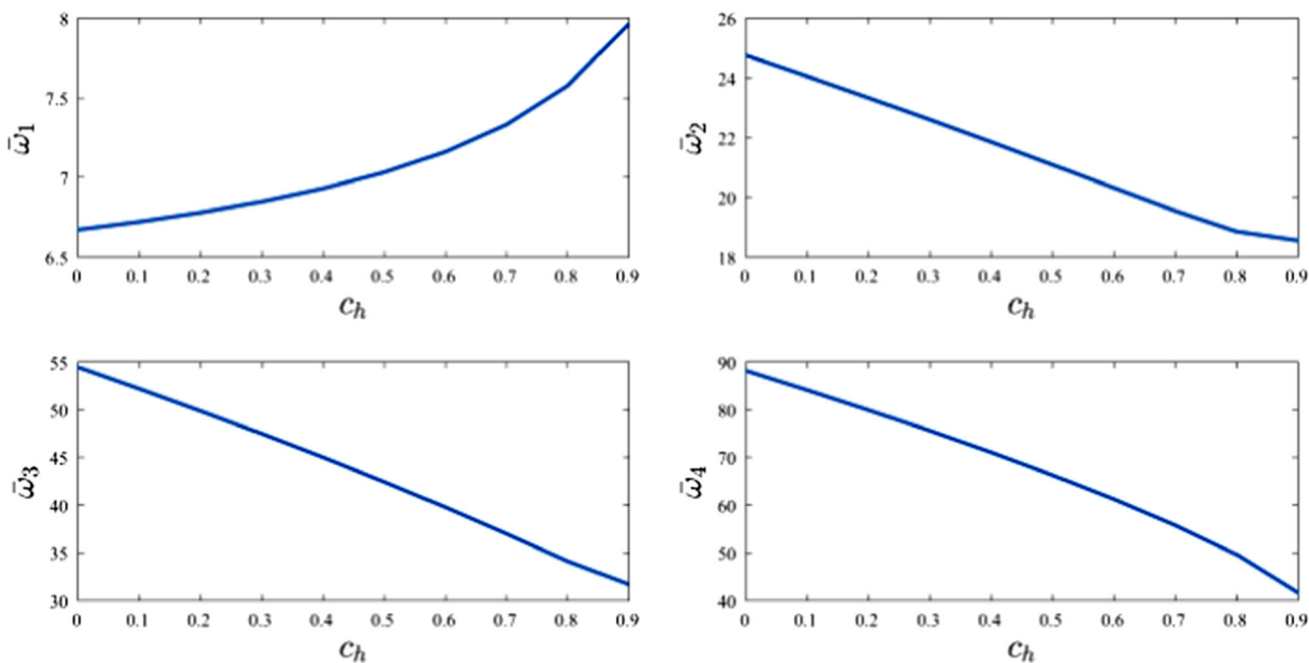


Fig. 10 Effect of the height taper ratio on the natural frequencies of a rotating double-tapered AFGM nanobeam

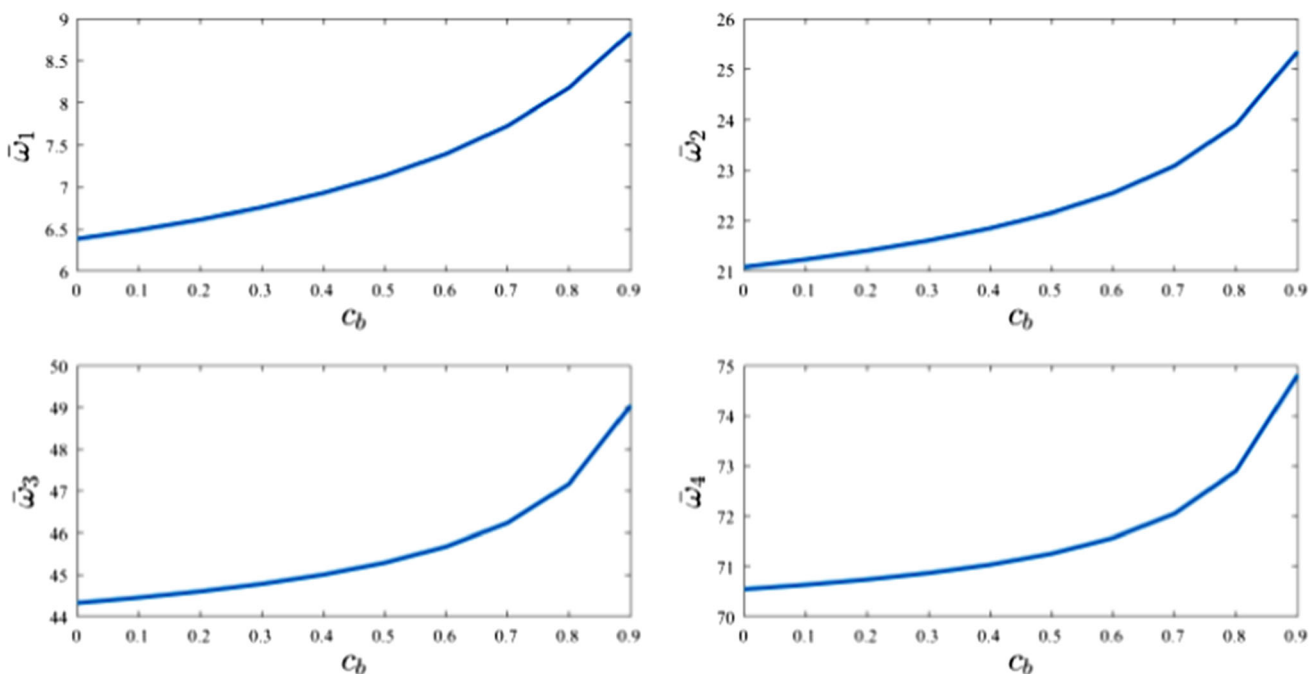


Fig. 11 Effect of the breadth taper ratio on the natural frequencies of a rotating double-tapered AFGM nanobeam

first four dimensionless natural frequencies. Additionally, here it is seen that higher modes appear when more terms are taken into account in DTM application. Thus, depending on the order of the required mode, one must try a few values for the term number at the beginning of the numerical calculations in order to find an adequate number of terms.

Table 8 shows the first four dimensionless natural frequencies of a rotating double-tapered AFGM nanobeam. Figure 7 shows the corresponding mode shapes of those natural frequencies obtained from Eq. (45).

Figure 8 shows the importance of considering the non-local Eringen theory and specifically the nonlocal scaling parameter in analyzing a nanobeam system. It can be seen

that increasing τ causes an increase in the first natural frequency and a decrease in the remaining three. As $\tau = 0$, shows the behavior of the nanobeam with classical Euler–Bernoulli theory, the natural frequencies are different when the nonlocal parameter is being counted and it shows the importance of this parameter. The most interesting result is that the importance of this parameter becomes clearer when the attention is directed towards the higher natural frequencies.

The effects of rotational speed and hub radius on natural frequencies were investigated and the results are shown in Figure 9. It was seen that by increasing rotational speed, the natural frequencies increase and this trend is also occurring when the hub radius increases. In addition, rotational speed and hub radius have more impact on the higher natural frequencies than the lower ones and the rate of changing the natural frequencies due to changing those two parameters is more evident on the higher natural frequencies as well. It is noted that natural frequencies remain constant by changing hub radius for a non-rotating double-tapered AFGM nanobeam which makes sense, because without rotation there is no centrifugal force applied to the nanobeam, and the only important relationship between the hub and the nanobeam is the boundary conditions between them.

The proposed nanobeam tapered linearly from both its height and breadth. The results of this tapering effect from its height are plotted in Figure 10. As it is very obvious from Eq. (16), c_h can be between 0 to 1. From the results, it can be understood that by increasing the height taper ratio, or in the other words by making it tapered quicker, the first natural frequency increases but the other ones decrease. This trend of changing in the value of natural frequencies due to the changing in height taper ratio is more evident when it gets to the higher natural frequencies.

Based on Eq. (15), c_b can be between 0 to 1. Therefore, the effect of the breadth taper ratio on the natural frequencies is shown in Fig. 11. It must be emphasized that by increasing the breadth taper ratio the natural frequencies increase.

Looking at the results of the effect of height and breadth taper ratio on the natural frequencies, it can be concluded that by increasing mode number, the effect of height taper ratio on the natural frequencies becomes more dominant than the effect of breadth taper ratio. In other words, the height taper ratio plays a key role compared to the breadth taper ratio when the mode number increases.

8 Conclusion

In this article, free vibration analysis of a rotating double-tapered AFGM nanobeam was presented. It was assumed that the height and the breadth of nanobeam taper linearly along its length and moreover, the mechanical properties of it change nonlinearly along its length. Using the nonlocal Eringen theory, the equation of motion of the proposed system and the boundary conditions were developed. Afterward, the separation of variables solution was applied to obtain an equation containing the frequency. Then, DTM and related rules were employed to convert the obtained equation as well as the boundary conditions to the form of algebraic equations, from which, a characteristic equation was extracted. Solving the resultant characteristic equation yielded the dimensionless natural frequencies. Additionally, the corresponding mode shapes were obtained and the effect of several parameters such as nonlocal scaling parameter, rotational speed, hub radius, height and breadth taper ratios were investigated on the natural frequencies and the results were presented. Finally, the results were compared with those reported in the literature and an excellent agreement was observed. Moreover, the following results were obtained for a rotating double-tapered AFGM nanobeam system;

- The value of the first natural frequency is increased by increasing the nonlocal scaling parameter and the rest is decreased.
- The importance of the nonlocal scaling parameter becomes clearer when the attention is directed towards the higher natural frequencies.
- Increasing rotational speed and hub radius cause an increase in the natural frequencies.
- Rotational speed, hub radius, and height taper ratio have more impact on the higher natural frequencies than the lower ones and the rate of changing the natural frequencies due to changing those parameters is more evident.
- Increasing the breadth taper ratio causes an increase in the natural frequencies. Moreover, increasing the height taper ratio causes an increase in the first natural frequency but a decrease in the rest.

The results given in this paper present some complementary information about the exact size-dependent vibration behavior of the rotating cantilever double-tapered AFGM nanobeams. Therefore, the paper and its results can be applicable in an efficient design of the nano-structures in which the rotating nanobeams play a pivotal role.

Acknowledgements This research is supported by the Australian Research Council (ARC) Discovery Project (DP) Grant, and the

Australian Research Council (ARC) Linkage Infrastructure, Equipment and Facilities (LIEF) grant.

Appendix A

Coefficients of the centrifugal force (Eq. 19)

$$\begin{aligned}
 A_1 &= A_0 \Omega^2 \rho_L R \\
 A_2 &= \frac{A_0 \Omega^2 \rho_L}{2} \left[1 - (c_b + c_h) \frac{R}{L} \right] \\
 A_3 &= \frac{A_0 \Omega^2}{3} \left[\rho_L \left(\frac{c_b c_h R}{L^2} - \frac{c_b + c_h}{L} \right) - \frac{R}{L^2} (\rho_L - \rho_R) \right] \\
 A_4 &= \frac{A_0 \Omega^2}{4L^2} \left[\rho_L c_b c_h - (\rho_L - \rho_R) \left(1 - (c_b + c_h) \frac{R}{L} \right) \right] \\
 A_5 &= -\frac{A_0 \Omega^2 (\rho_L - \rho_R)}{5L^2} \left[\frac{c_b c_h R}{L^2} - \frac{c_b + c_h}{L} \right] \\
 A_6 &= -\frac{A_0 \Omega^2 (\rho_L - \rho_R)}{6L^4} [c_b c_h]
 \end{aligned}$$

Appendix B

Function coefficients of the equation of motion of the dynamical system (Eq. 20)

$$\begin{aligned}
 B_1 &= A_0 \left\{ \rho_L - (\rho_L - \rho_R) \frac{x^2}{L^2} \right\} \left\{ 1 - (c_b + c_h) \frac{x}{L} + c_b c_h \frac{x^2}{L^2} \right\} \\
 &\quad + 2A_0 (\rho_L - \rho_R) \frac{(e_0 a)^2}{L^2} \left\{ 1 - (c_b + c_h) \frac{x}{L} + c_b c_h \frac{x^2}{L^2} \right\} \\
 &\quad + 4A_0 (\rho_L - \rho_R) \frac{(e_0 a)^2 x}{L^2} \left\{ c_b \left(c_h \frac{x}{L} - 1 \right) + c_h \left(c_b \frac{x}{L} - 1 \right) \right\} \\
 &\quad - 2A_0 c_b c_h \frac{(e_0 a)^2}{L^2} \left\{ \rho_L - (\rho_L - \rho_R) \frac{x^2}{L^2} \right\} \\
 B_2 &= I_{y_0} \left(c_b \frac{x}{L} - 1 \right) \left(c_h \frac{x}{L} - 1 \right)^3 \left\{ E_L - (E_L - E_R) \frac{x^2}{L^2} \right\} \\
 &\quad + (e_0 a)^2 \{ A_1 L + A_2 L^2 + A_3 L^3 + A_4 L^4 + A_5 L^5 + A_6 L^6 \} \\
 &\quad - (e_0 a)^2 \{ A_1 x + A_2 x^2 + A_3 x^3 + A_4 x^4 + A_5 x^5 + A_6 x^6 \}
 \end{aligned}$$

$$\begin{aligned}
 B_3 &= -4I_{y_0} x \left(c_b \frac{x}{L} - 1 \right) \left(c_h \frac{x}{L} - 1 \right)^3 \frac{(E_L - E_R)}{L^2} \\
 &\quad + \frac{2I_{y_0}}{L} \left\{ E_L - (E_L - E_R) \frac{x^2}{L^2} \right\} \left\{ c_b \left(c_h \frac{x}{L} - 1 \right)^3 \right. \\
 &\quad \left. + 3c_h \left(c_b \frac{x}{L} - 1 \right) \left(c_h \frac{x}{L} - 1 \right)^2 \right\} - (e_0 a)^2 \\
 &\quad \{ 18A_6 x^5 + 15A_5 x^4 + 12A_4 x^3 + 9A_3 x^2 + 6A_2 x + 3A_1 \}
 \end{aligned}$$

$$\begin{aligned}
 B_4 &= -2I_{y_0} \left(c_b \frac{x}{L} - 1 \right) \left(c_h \frac{x}{L} - 1 \right)^3 \frac{(E_L - E_R)}{L^2} - 4x \frac{(E_L - E_R)}{L^3} \\
 &\quad \left\{ I_{y_0} c_b \left(c_h \frac{x}{L} - 1 \right)^3 + 3I_{y_0} c_h \left(c_b \frac{x}{L} - 1 \right) \left(c_h \frac{x}{L} - 1 \right)^2 \right\} \\
 &\quad + \frac{6I_{y_0}}{L^2} \left\{ c_h^2 \left(1 - (c_b + c_h) \frac{x}{L} + c_b c_h \frac{x^2}{L^2} \right) + c_b c_h \left(c_h \frac{x}{L} - 1 \right)^2 \right\} \\
 &\quad \left\{ E_L - (E_L - E_R) \frac{x^2}{L^2} \right\} \\
 &\quad - \{ A_1 L + A_2 L^2 + A_3 L^3 + A_4 L^4 + A_5 L^5 + A_6 L^6 \} \\
 &\quad + \{ A_1 x + A_2 x^2 + A_3 x^3 + A_4 x^4 + A_5 x^5 + A_6 x^6 \} \\
 &\quad - (e_0 a)^2 \{ 90A_6 x^4 + 60A_5 x^3 + 36A_4 x^2 + 18A_3 x + 6A_2 \}
 \end{aligned}$$

$$\begin{aligned}
 B_5 &= \{ A_1 + 2A_2 x + 3A_3 x^2 + 4A_4 x^3 + 5A_5 x^4 + 6A_6 x^5 \} \\
 &\quad - (e_0 a)^2 \{ 120A_6 x^3 + 60A_5 x^2 + 24A_4 x + 6A_3 \}
 \end{aligned}$$

$$\begin{aligned}
 B_6 &= 4A_0 (\rho_L - \rho_R) \frac{(e_0 a)^2}{L^2} \left\{ x - (c_b + c_h) \frac{x^2}{L} + c_b c_h \frac{x^3}{L^2} \right\} \\
 &\quad - \frac{2A_0 (e_0 a)^2}{L} \left\{ c_b \left(c_h \frac{x}{L} - 1 \right) + c_h \left(c_b \frac{x}{L} - 1 \right) \right\} \\
 &\quad \left\{ \rho_L - (\rho_L - \rho_R) \frac{x^2}{L^2} \right\}
 \end{aligned}$$

$$\begin{aligned}
 B_7 &= -A_0 (e_0 a)^2 \left\{ 1 - (c_b + c_h) \frac{x}{L} + c_b c_h \frac{x^2}{L^2} \right\} \\
 &\quad \left\{ \rho_L - (\rho_L - \rho_R) \frac{x^2}{L^2} \right\}
 \end{aligned}$$

Appendix C

Function coefficients of the dimensionless equation of motion of the dynamical system (Eq. 27)

$$\begin{aligned}
 C_0 &= \frac{L^3}{E_L I_{y_0}} \left\{ \begin{aligned} &A_0 \rho_L (-\omega^2) L + \left\{ -2A_0 c_b c_h \frac{(e_0 a)^2}{L^2} \rho_L (-\omega^2) L \right\} + \left\{ 2A_0 (\rho_L - \rho_R) \frac{(e_0 a)^2}{L^2} (-\omega^2) L \right\} + \\ &\left[-A_0 \rho_L (c_b + c_h) (-\omega^2) L - 6A_0 (\rho_L - \rho_R) \frac{(e_0 a)^2}{L^2} (c_b + c_h) (-\omega^2) L \right] \bar{x} + \\ &\left[A_0 \{ \rho_L c_b c_h - (\rho_L - \rho_R) \} (-\omega^2) L + 12A_0 (\rho_L - \rho_R) \frac{(e_0 a)^2}{L^2} c_b c_h (-\omega^2) L \right] \bar{x}^2 + \\ &[A_0 (c_b + c_h) (\rho_L - \rho_R) (-\omega^2) L] \bar{x}^3 + [-A_0 c_b c_h (\rho_L - \rho_R) (-\omega^2) L] \bar{x}^4 \end{aligned} \right\} \\
 C_1 &= \frac{L^3}{E_L I_{y_0}} \left\{ \begin{aligned} &A_1 + 2A_2 L \bar{x} + 3A_3 L^2 \bar{x}^2 + 4A_4 L^3 \bar{x}^3 + 5A_5 L^4 \bar{x}^4 + 6A_6 L^5 \bar{x}^5 + \\ &\frac{(e_0 a)^2}{L^2} \left\{ 2A_0 L (c_b + c_h) \rho_L (-\omega^2) + \{ -4A_0 L \rho_L c_b c_h (-\omega^2) + 4A_0 (\rho_L - \rho_R) L (-\omega^2) \} \bar{x} - \right. \\ &\quad \left. 6A_0 (\rho_L - \rho_R) (c_b + c_h) L (-\omega^2) \bar{x}^2 + 8A_0 (\rho_L - \rho_R) c_b c_h L (-\omega^2) \bar{x}^3 \right. \\ &\quad \left. \frac{(e_0 a)^2}{L^2} \{ -120A_6 L^5 \bar{x}^3 - 60A_5 L^4 \bar{x}^2 - 24A_4 L^3 \bar{x} - 6A_3 L^2 \} \right\} + \end{aligned} \right\} \\
 C_2 &= \frac{L^3}{E_L I_{y_0}} \left\{ \begin{aligned} &\left\{ -I_{y_0} \frac{2(E_L - E_R)}{L^3} + \frac{6I_{y_0}}{L^3} (c_b c_h + c_h^2) E_L \right\} + \left\{ -\frac{6I_{y_0}}{L^3} (3c_b c_h^2 + c_h^3) E_L + 6 \frac{(E_L - E_R)}{L^3} I_{y_0} (3c_h + c_b) \right\} \bar{x} + \\ &\frac{6I_{y_0}}{L^3} \{ 2c_b c_h^3 E_L - 6(c_b c_h + c_h^2) (E_L - E_R) \} \bar{x}^2 + 20 \frac{(E_L - E_R)}{L^3} I_{y_0} c_h (3c_b c_h + c_h^2) \bar{x}^3 - \\ &30 \frac{(E_L - E_R)}{L^3} I_{y_0} c_b c_h^3 \bar{x}^4 - \{ A_1 + A_2 L + A_3 L^2 + A_4 L^3 + A_5 L^4 + A_6 L^5 \} + \\ &\quad \{ A_1 \bar{x} + A_2 L \bar{x}^2 + A_3 L^2 \bar{x}^3 + A_4 L^3 \bar{x}^4 + A_5 L^4 \bar{x}^5 + A_6 L^5 \bar{x}^6 \} + \\ &\frac{A_0 (e_0 a)^2}{L^2} \left\{ -L \rho_L (-\omega^2) + L \rho_L (c_b + c_h) (-\omega^2) \bar{x} - L \{ \rho_L c_b c_h - (\rho_L - \rho_R) \} (-\omega^2) \bar{x}^2 - \right. \\ &\quad \left. L (c_b + c_h) (\rho_L - \rho_R) (-\omega^2) \bar{x}^3 + L c_b c_h (\rho_L - \rho_R) (-\omega^2) \bar{x}^4 \right\} + \\ &\frac{(e_0 a)^2}{L^2} \{ -90A_6 L^5 \bar{x}^4 - 60A_5 L^4 \bar{x}^3 - 36A_4 L^3 \bar{x}^2 - 18A_3 L^2 \bar{x} - 6A_2 L \} \end{aligned} \right\} \\
 C_3 &= \frac{L^3}{E_L I_{y_0}} \left\{ \begin{aligned} &-I_{y_0} \frac{4(E_L - E_R)}{L^3} \bar{x} - \frac{12I_{y_0}}{L^3} (E_L - E_R) c_b c_h^3 \bar{x}^5 + \\ &\frac{10I_{y_0}}{L^3} (E_L - E_R) c_h (3c_b c_h + c_h^2) \bar{x}^4 + \frac{2I_{y_0}}{L^3} \{ 4E_L c_b c_h^3 - 12(E_L - E_R) c_h (c_b + c_h) \} \bar{x}^3 + \\ &\frac{2I_{y_0}}{L^3} \{ -3E_L c_h (3c_b c_h + c_h^2) + 3(E_L - E_R) (3c_h + c_b) \} \bar{x}^2 + \frac{12I_{y_0}}{L^3} E_L c_h (c_b + c_h) \bar{x} - \\ &\frac{2I_{y_0}}{L^3} E_L (3c_h + c_b) + \frac{(e_0 a)^2}{L^2} \{ -18A_6 L^5 \bar{x}^5 - 15A_5 L^4 \bar{x}^4 - 12A_4 L^3 \bar{x}^3 - 9A_3 L^2 \bar{x}^2 - 6A_2 L \bar{x} - 3A_1 \} \end{aligned} \right\} \\
 C_4 &= \frac{L^3}{E_L I_{y_0}} \left\{ \begin{aligned} &\frac{I_{y_0}}{L^3} E_L - \frac{I_{y_0}}{L^3} E_L (c_b + 3c_h) \bar{x} + \frac{I_{y_0}}{L^3} \{ 3E_L c_h (c_b + c_h) - (E_L - E_R) \} \bar{x}^2 + \\ &\frac{I_{y_0}}{L^3} \{ (E_L - E_R) (c_b + 3c_h) - E_L c_h^2 (3c_b + c_h) \} \bar{x}^3 + \\ &\frac{I_{y_0}}{L^3} \{ E_L c_b c_h^3 - 3(E_L - E_R) c_h (c_b + c_h) \} \bar{x}^4 + \\ &\frac{I_{y_0}}{L^3} (E_L - E_R) c_h^2 (3c_b + c_h) \bar{x}^5 - \frac{I_{y_0}}{L^3} (E_L - E_R) c_b c_h^3 \bar{x}^6 - \\ &\frac{(e_0 a)^2}{L^2} \{ A_1 \bar{x} + A_2 L \bar{x}^2 + A_3 L^2 \bar{x}^3 + A_4 L^3 \bar{x}^4 + A_5 L^4 \bar{x}^5 + A_6 L^5 \bar{x}^6 \} + \\ &\frac{(e_0 a)^2}{L^2} \{ A_1 + A_2 L + A_3 L^2 + A_4 L^3 + A_5 L^4 + A_6 L^5 \} \end{aligned} \right\}
 \end{aligned}$$

Appendix D

Function coefficients of the dimensionless bending moment
(Eq. 30)

$$D_0 = \frac{L}{E_L I_{y_0}} \left\{ (e_0 a)^2 \left[(A_0 L \rho_L (-\omega^2) - A_0 L (\rho_L - \rho_R) (-\omega^2) \bar{x}^2) (1 - (c_b + c_h) \bar{x} + c_b c_h \bar{x}^2) \right] \right\}$$

$$D_1 = \frac{L}{E_L I_{y_0}} \left\{ (e_0 a)^2 \left[6A_6 (L \bar{x})^5 + 5A_5 (L \bar{x})^4 + 4A_4 (L \bar{x})^3 + 3A_3 (L \bar{x})^2 + 2A_2 L \bar{x} + A_1 \right] \right\}$$

$$D_2 = \frac{L}{E_L I_{y_0}} \left\{ \left(-\frac{I_{y_0} E_L}{L} + \frac{I_{y_0} (E_L - E_R) \bar{x}^2}{L} \right) \left(1 - (c_b + 3c_h) \bar{x} + 3(c_b + c_h) c_h \bar{x}^2 - \frac{(c_h)^2 (c_h + 3c_b) \bar{x}^3 + c_b (c_h)^3 \bar{x}^4}{(c_h)^2 (c_h + 3c_b) \bar{x}^3 + c_b (c_h)^3 \bar{x}^4} \right) + \right. \\ \left. (e_0 a)^2 \left\{ (A_1 \bar{x} + A_2 L (\bar{x})^2 + A_3 L^2 (\bar{x})^3 + A_4 L^3 (\bar{x})^4 + A_5 L^4 (\bar{x})^5 + A_6 L^5 (\bar{x})^6) \right\} \right\}$$

Appendix E

Function coefficients of the dimensionless shear force
(Eq. 31)

$$E_0 = \frac{L^2}{E_L I_{y_0}} \left\{ \frac{(e_0 a)^2}{L} \left[A_0 \rho_L (-\omega^2) L (-c_b + c_h) + 2c_b c_h \bar{x} - A_0 (\rho_L - \rho_R) (-\omega^2) L (2\bar{x} - 3(c_b + c_h) \bar{x}^2 + 4c_b c_h \bar{x}^3) \right] \right\}$$

$$E_1 = \frac{L^2}{E_L I_{y_0}} \left\{ \frac{(e_0 a)^2}{L} \left[(A_0 \rho_L (-\omega^2) L - A_0 (\rho_L - \rho_R) (-\omega^2) L \bar{x}^2) (1 - (c_b + c_h) \bar{x} + c_b c_h \bar{x}^2) + \right. \right. \\ \left. \left. (30A_6 (L)^5 \bar{x}^4 + 20A_5 (L)^4 \bar{x}^3 + 12A_4 (L)^3 \bar{x}^2 + 6A_3 (L)^2 \bar{x} + 2A_2 L) \right] \right\}$$

$$E_2 = \frac{L^2}{E_L I_{y_0}} \left\{ \frac{-\frac{I_{y_0} E_L}{L^2} (-c_b + 3c_h) + 6(c_b + c_h) c_h \bar{x} - 3(c_h)^2 (c_h + 3c_b) \bar{x}^2 + 4c_b (c_h)^3 \bar{x}^3}{L^2} \right. \\ \left. + \frac{I_{y_0} (E_L - E_R)}{L^2} (2\bar{x} - 3(c_b + 3c_h) \bar{x}^2 + 12(c_b + c_h) c_h \bar{x}^3 - 5(c_h)^2 (c_h + 3c_b) \bar{x}^4 + 6c_b (c_h)^3 \bar{x}^5) + \right. \\ \left. \frac{2(e_0 a)^2}{L} (A_1 + 2A_2 L \bar{x} + 3A_3 L^2 (\bar{x})^2 + 4A_4 L^3 (\bar{x})^3 + 5A_5 L^4 (\bar{x})^4 + 6A_6 L^5 (\bar{x})^5) \right\}$$

$$E_3 = \frac{L^2}{E_L I_{y_0}} \left\{ \left(-\frac{I_{y_0} E_L}{L^2} + \frac{I_{y_0} (E_L - E_R) \bar{x}^2}{L^2} \right) \left(1 - (c_b + 3c_h) \bar{x} + 3(c_b + c_h) c_h \bar{x}^2 - \frac{(c_h)^2 (c_h + 3c_b) \bar{x}^3 + c_b (c_h)^3 \bar{x}^4}{(c_h)^2 (c_h + 3c_b) \bar{x}^3 + c_b (c_h)^3 \bar{x}^4} \right) + \right. \\ \left. (e_0 a)^2 \left\{ (A_1 \bar{x} + A_2 L (\bar{x})^2 + A_3 L^2 (\bar{x})^3 + A_4 L^3 (\bar{x})^4 + A_5 L^4 (\bar{x})^5 + A_6 L^5 (\bar{x})^6) \right\} \right\}$$

Appendix F

Function coefficients of the transformed dimensionless equation of motion of the dynamical system (Eq. 35)

$$\begin{aligned}
 F_1 &= \frac{L^3}{E_L I_{y_0}} \left\{ -A_0 c_b c_h (\rho_L - \rho_R) (-\omega^2) L + A_6 L^5 (m - 4)(m - 5) + 6A_6 L^5 (m - 4) \right\} \\
 F_2 &= \frac{L^3}{E_L I_{y_0}} \left\{ A_0 (c_b + c_h) (\rho_L - \rho_R) (-\omega^2) L + 5A_5 L^4 (m - 3) + A_5 L^4 (m - 3)(m - 4) \right\} \\
 F_3 &= \frac{L^3}{E_L I_{y_0}} \left\{ \begin{aligned} & A_0 \{ \rho_L c_b c_h - (\rho_L - \rho_R) \} (-\omega^2) L - 30 \frac{(E_L - E_R)}{L^3} I_{y_0} c_b c_h^3 (m - 3)(m - 2) - \\ & \frac{12 I_{y_0}}{L^3} (E_L - E_R) c_b c_h^3 (m - 2)(m - 3)(m - 4) - \\ & \frac{I_{y_0}}{L^3} (E_L - E_R) c_b c_h^3 (m - 2)(m - 3)(m - 4)(m - 5) + 4A_4 L^3 (m - 2) + A_4 L^3 (m - 2)(m - 3) + \\ & 12A_0 (\rho_L - \rho_R) \frac{(e_0 a)^2}{L} c_b c_h (-\omega^2) + 8A_0 (\rho_L - \rho_R) \frac{(e_0 a)^2}{L} c_b c_h (-\omega^2) (m - 2) + \\ & A_0 (e_0 a)^2 c_b c_h (\rho_L - \rho_R) (-\omega^2) \frac{1}{L} (m - 2)(m - 3) - 120 (e_0 a)^2 A_6 L^3 (m - 2) - \\ & 90 (e_0 a)^2 A_6 L^3 (m - 2)(m - 3) - 18 (e_0 a)^2 A_6 L^3 (m - 3)(m - 4)(m - 2) - \\ & (e_0 a)^2 A_6 L^3 (m - 4)(m - 5)(m - 3)(m - 2) \end{aligned} \right\} \\
 F_4 &= \frac{L^3}{E_L I_{y_0}} \left\{ \begin{aligned} & -A_0 \rho_L (c_b + c_h) (-\omega^2) L + 20 \frac{(E_L - E_R)}{L^3} I_{y_0} c_h (3c_b c_h + c_h^2) (m - 1)(m - 2) + \\ & \frac{10 I_{y_0}}{L^3} (E_L - E_R) c_h (3c_b c_h + c_h^2) (m - 1)(m - 2)(m - 3) + \\ & \frac{I_{y_0}}{L^3} (E_L - E_R) c_h^2 (3c_b + c_h) (m - 1)(m - 2)(m - 3)(m - 4) + \\ & 3A_3 L^2 (m - 1) + A_3 L^2 (m - 1)(m - 2) - 6A_0 (\rho_L - \rho_R) \frac{(e_0 a)^2}{L} (c_b + c_h) (-\omega^2) - \\ & 6A_0 (\rho_L - \rho_R) \frac{(e_0 a)^2}{L} (c_b + c_h) (-\omega^2) (m - 1) - \\ & A_0 \frac{(e_0 a)^2}{L} (c_b + c_h) (\rho_L - \rho_R) (-\omega^2) (m - 2)(m - 1) - 60 (e_0 a)^2 A_5 L^2 (m - 1) - \\ & 60 (e_0 a)^2 A_5 L^2 (m - 2)(m - 1) - 15 (e_0 a)^2 A_5 L^2 (m - 3)(m - 1)(m - 2) - \\ & (e_0 a)^2 A_5 L^2 (m - 4)(m - 1)(m - 3)(m - 2) \end{aligned} \right\} \\
 F_5 &= \frac{L^3}{E_L I_{y_0}} \left\{ \begin{aligned} & A_0 \rho_L (-\omega^2) L + \frac{6 I_{y_0}}{L^3} \{ 2c_b c_h^3 E_L - 6(c_b c_h + c_h^2) (E_L - E_R) \} (m - 1)(m) + \\ & \frac{2 I_{y_0}}{L^3} \{ 4E_L c_b c_h^3 - 12(E_L - E_R) c_h (c_b + c_h) \} (m)(m - 1)(m - 2) + \\ & \frac{I_{y_0}}{L^3} \{ E_L c_b c_h^3 - 3(E_L - E_R) c_h (c_b + c_h) \} (m)(m - 2)(m - 1)(m - 3) + \\ & 2A_2 L(m) + A_2 L(m)(m - 1) + 2A_0 (\rho_L - \rho_R) \frac{(e_0 a)^2}{L} (-\omega^2) + \\ & 4A_0 (\rho_L - \rho_R) \frac{(e_0 a)^2}{L} (-\omega^2) m - 2A_0 c_b c_h \frac{(e_0 a)^2}{L} \rho_L (-\omega^2) - 4A_0 \frac{(e_0 a)^2}{L} \rho_L c_b c_h (-\omega^2) m - \\ & A_0 \frac{(e_0 a)^2}{L} \{ \rho_L c_b c_h - (\rho_L - \rho_R) \} (-\omega^2) (m - 1)(m) - 24 (e_0 a)^2 A_4 L(m) - \\ & 36 (e_0 a)^2 A_4 L(m)(m - 1) - 12 (e_0 a)^2 A_4 L(m)(m - 1)(m - 2) - \\ & (e_0 a)^2 A_4 L(m)(m - 1)(m - 3)(m - 2) \end{aligned} \right\}
 \end{aligned}$$

$$\begin{aligned}
 F_6 &= \frac{L^3}{E_L I_{y_0}} \left\{ \begin{aligned} &6 \frac{(E_L - E_R)}{L^3} I_{y_0} (3c_h + c_b)(m+1)(m) - \frac{6I_{y_0}}{L^3} (3c_b c_h^2 + c_h^3) E_L (m+1)(m) + \\ &\frac{2I_{y_0}}{L^3} \{-3E_L c_h (3c_b c_h + c_h^2) + 3(E_L - E_R)(3c_h + c_b)\} (m+1)(m)(m-1) + \\ &\frac{I_{y_0}}{L^3} \{(E_L - E_R)(c_b + 3c_h) - E_L c_h^2 (3c_b + c_h)\} (m+1)(m-2)(m-1)(m) + A_1(m+1) + \\ &A_1(m+1)(m) + 2A_0 \frac{(e_0 a)^2}{L} (c_b + c_h) \rho_L (-\omega^2)(m+1) + \\ &A_0 \frac{(e_0 a)^2}{L} \rho_L (c_b + c_h) (-\omega^2)(m)(m+1) - 6(e_0 a)^2 A_3(m+1) - \\ &18(e_0 a)^2 A_3(m)(m+1) - 9(e_0 a)^2 A_3(m)(m-1)(m+1) - \\ &(e_0 a)^2 A_3(m)(m-1)(m+1)(m-2) \end{aligned} \right\} \\
 F_7 &= \frac{L^3}{E_L I_{y_0}} \left\{ \begin{aligned} &-I_{y_0} \frac{2(E_L - E_R)}{L^3} (m+2)(m+1) - I_{y_0} \frac{4(E_L - E_R)}{L^3} (m+2)(m+1)(m) + \\ &\frac{6I_{y_0}}{L^3} (c_b c_h + c_h^2) E_L (m+2)(m+1) + \frac{12I_{y_0}}{L^3} E_L c_h (c_b + c_h)(m+2)(m+1)(m) + \\ &\frac{I_{y_0}}{L^3} \{3E_L c_h (c_b + c_h) - (E_L - E_R)\} (m+2)(m+1)(m-1)(m) - \\ &\{A_1 + A_2 L + A_3 L^2 + A_4 L^3 + A_5 L^4 + A_6 L^5\} (m+2)(m+1) - \\ &A_0 \frac{(e_0 a)^2}{L} \rho_L (-\omega^2)(m+2)(m+1) - 6 \frac{(e_0 a)^2}{L} A_2(m+2)(m+1) - \\ &6 \frac{(e_0 a)^2}{L} A_2(m)(m+2)(m+1) - \frac{(e_0 a)^2}{L} A_2(m)(m-1)(m+2)(m+1) \end{aligned} \right\} \\
 F_8 &= \frac{L^3}{E_L I_{y_0}} \left\{ \begin{aligned} &-\frac{2I_{y_0}}{L^3} E_L (3c_h + c_b)(m+3)(m+2)(m+1) - \\ &\frac{I_{y_0}}{L^3} E_L (c_b + 3c_h)(m+3)(m+2)(m+1)(m) - 3 \frac{(e_0 a)^2}{L^2} A_1(m+3)(m+2)(m+1) - \\ &\frac{(e_0 a)^2}{L^2} A_1(m)(m+3)(m+2)(m+1) \end{aligned} \right\} \\
 F_9 &= \frac{L^3}{E_L I_{y_0}} \left\{ \begin{aligned} &\frac{I_{y_0}}{L^3} E_L (m+4)(m+3)(m+2)(m+1) + \\ &\frac{(e_0 a)^2}{L^2} \{A_1 + A_2 L + A_3 L^2 + A_4 L^3 + A_5 L^4 + A_6 L^5\} (m+4)(m+3)(m+2)(m+1) \end{aligned} \right\}
 \end{aligned}$$

Appendix G

Coefficients of the transformed dimensionless bending moment (Eq. 38)

$$G_1 = \frac{L}{E_L I_{y_0}} \left\{ -\frac{I_{y_0} E_R}{L} \left(1 - (c_b + 3c_h) + 3(c_b + c_h)c_h - (c_h)^2(c_h + 3c_b) + c_b(c_h)^3 \right) \right\}$$

$$G_2 = \frac{L}{E_L I_{y_0}} \{A_0 L \rho_R (-\omega^2)(1 - (c_b + c_h) + c_b c_h)\}$$

$$G_3 = \frac{L}{E_L I_{y_0}} \{6A_6 L^5 + 5A_5 L^4 + 4A_4 L^3 + 3A_3 L^2 + 2A_2 L + A_1\}$$

Appendix H

Coefficients of the transformed dimensionless shear force (Eq. 39)

$$H_1 = \frac{L^2}{E_L I_{y_0}} \left\{ -\frac{I_{y_0} E_R}{L^2} (1 - (c_b + 3c_h) + 3(c_b + c_h)c_h - (c_h)^2(c_h + 3c_b) + c_b(c_h)^3) \right\}$$

$$\begin{aligned}
 H_2 &= \frac{L^2}{E_L I_{y_0}} \left\{ \begin{aligned} &-\frac{I_{y_0} E_L}{L^2} \left(-(c_b + 3c_h) + 6(c_b + c_h)c_h - 3(c_h)^2(c_h + 3c_b) + 4c_b(c_h)^3 \right) + \\ &\frac{I_{y_0}(E_L - E_R)}{L^2} \left(2 - 3(c_b + 3c_h) + 12(c_b + c_h)c_h - 5(c_h)^2(c_h + 3c_b) + 6c_b(c_h)^3 \right) \end{aligned} \right\} \\
 H_3 &= \frac{L^2}{E_L I_{y_0}} \{ A_0 \rho_L (-\omega^2) (-c_b + c_h) + 2c_b c_h - A_0 (\rho_L - \rho_R) (-\omega^2) (2 - 3(c_b + c_h) + 4c_b c_h) \} \\
 H_4 &= \frac{L^2}{E_L I_{y_0}} \left\{ 2 \left(6A_6 L^4 + 5A_5 L^3 + 4A_4 L^2 + 3A_3 L + 2A_2 + \frac{A_1}{L} \right) \right\} \\
 H_5 &= \frac{L^2}{E_L I_{y_0}} \{ A_0 \rho_R (-\omega^2) (1 - (c_b + c_h) + c_b c_h) + (30A_6 L^4 + 20A_5 L^3 + 12A_4 L^2 + 6A_3 L + 2A_2) \}
 \end{aligned}$$

References

Aranda-Ruiz J, Loya J, Fernández-Sáez J (2012) Bending vibrations of rotating nonuniform nanocantilevers using the Eringen nonlocal elasticity theory. *Compos Struct* 94(9):2990–3001

Araujo dos Santos JV, Mota Soares CM (2012) Nonlocal material properties of single-walled carbon nanotubes. *International Journal of Smart and Nano Materials* 3(2):141–151

Aria AI, Friswell MI (2019) A nonlocal finite element model for buckling and vibration of functionally graded nanobeams. *Compos B Eng* 166:233–246

Aubad MJ, Khafaji SOW, Hussein MT, Al-Shujairi MA (2019) Modal analysis and transient response of axially functionally graded (AFG) beam using finite element method. *Mater Res Express* 6(10)

Aydin K (2013) Influence of Crack and Slenderness Ratio on the Eigenfrequencies of Euler-Bernoulli and Timoshenko Beams. *Mech Adv Mater Struct* 20(5):339–352

Aydogdu M (2014) A nonlocal rod model for axial vibration of double-walled carbon nanotubes including axial van der Waals force effects. *J Vib Control* 1–23

Duan WH, Wang CM, Zhang YY (2007) Calibration of nonlocal scaling effect parameter for free vibration of carbon nanotubes by molecular dynamics. *J Appl Phys* 101:024305

Eptameris KG, Koutsoumaris CC, Karyofyllis IG (2020) Eigenfrequencies of microtubules embedded in the cytoplasm by means of the nonlocal integral elasticity. *Acta Mech*

Eringen AC (1972) Linear theory of nonlocal elasticity and dispersion of plane waves. *Int J Eng Sci* 10(5):425–435

Eringen AC (1983) On differential-equations of nonlocal elasticity and solutions of screw dislocation and surface waves. *J Appl Phys* 54(9):4703–4710

Ghafarian M, Ariaei A (2016a) Free vibration analysis of a system of elastically interconnected rotating tapered Timoshenko beams using differential transform method. *Int J Mech Sci* 107:93–109

Ghafarian M, Ariaei A (2016b) Free vibration analysis of a multiple rotating nano-beams system based on the Eringen nonlocal elasticity theory. *J Appl Phys* 120:054301

Ghafarian M, Ariaei A (2019) Forced vibration analysis of a Timoshenko beam featuring bending-torsion on Pasternak foundation. *Appl Math Model* 66:472–485

Ghafarian M, Shirinzadeh B, Das TK, Al-Jodah A, Wei W (2018) Design of a novel parallel monolithic 6-DOF compliant micromanipulation mechanism. In: *Proceedings of the 2018 IEEE/ASME international conference on advanced intelligent mechatronics (AIM)*, Auckland, New Zealand, July 9–12, pp 997–1002

Ghafarian M, Shirinzadeh B, Al-Jodah A, Das TK, Wei W, Tian Y, Zhang D (2019) Design of a novel parallel monolithic 3-DOF compliant micromanipulator. In: *2019 International conference on manipulation, automation and robotics at small scales (MARSS)*, pp 1–6

Gholipour A, Ghayesh MH (2020) A coupled nonlinear nonlocal strain gradient theory for functionally graded Timoshenko nanobeams. *Microsyst Technol*. <https://doi.org/10.1007/s00542-020-04757-1>

Godara RK, Joglekar MM (2017) Alleviation of residual oscillations in electrostatically actuated variable-width microbeams using a feedforward control strategy. *Microsyst Technol* 23:4441–4457

Gorgani HH, Adeli MM, Hosseini M (2019) Pull-in behavior of functionally graded micro/nano-beams for MEMS and NEMS switches. *Microsyst Technol* 25:3165–3173

Gu Y, Chen X, Lin J, Lu M, Lu F, Zhang Z, Yang H (2018) Vibration-Assisted Roll-Type Polishing System Based on Compliant Micro-Motion Stage. *Micromachines* 9(10):499

Kikidis ML, Papadopoulos CA (1992) Slenderness ratio effect on cracked beam. *J Sound Vib* 155(1):1–11

Lin HP, Ro J (2003) Vibration analysis of planar serial-frame structures. *J Sound Vib* 262(5):1113–1131

Lin HP, Wu JD (2005) Dynamic analysis of planar closed-frame structures. *J Sound Vib* 282:249–264

Jha AK, Dasgupta SS (2019) Fractional order PID based optimal control for fractionally damped nonlocal nanobeam via genetic algorithm. *Microsyst Technol* 25:4291–4302

Karamanli A (2018) Free vibration analysis of two directional functionally graded beams using a third order shear deformation theory. *Compos Struct* 189:127–136

Moutlana MK, Adali S (2019) Fundamental frequencies of a torsional cantilever nano beam for dynamic atomic force microscopy (dAFM) in tapping mode. *Microsyst Technol* 25:1087–1098

- Noghrehabadi A, Ghalambaz M, Ghanbarzadeh A (2012) A new approach to the electrostatic pull-in instability of nanocantilever actuators using the ADM–Padé technique. *Comput Math Appl* 64(9):2806–2815
- Pinskier J, Shirinzadeh B (2019) Topology optimization of leaf flexures to maximize in-plane to out-of-plane compliance ratio. *Precision Eng* 55:397–407
- Ragb O, Mohamed M, Matbuly MS (2019) Free vibration of a piezoelectric nanobeam resting on nonlinear Winkler–Pasternak foundation by quadrature methods. *Heliyon* 5(6):e01856
- Rajasekaran S (2013) Differential transformation and differential quadrature methods for centrifugally stiffened axially functionally graded tapered beams. *Int J Mech Sci* 74:15–31
- Rastehkenari SF (2019) Random vibrations of functionally graded nanobeams based on unified nonlocal strain gradient theory. *Microsyst Technol* 25:691–704
- Ruocco E, Zhang H, Wang CM (2018) Buckling and vibration analysis of nonlocal axially functionally graded nanobeams based on Hencky-bar chain model. *Appl Math Model* 63:445–463
- Semnani SJ, Attarnejad R, Firouzjaei RK (2013) Free vibration analysis of variable thickness thin plates by two-dimensional differential transform method. *Acta Mech* 224:1643–1658
- Shahba A, Attarnejad R, Zarrinzadeh H (2013) Free vibration analysis of centrifugally stiffened tapered functionally graded beams. *Mech Adv Mater Struct* 20(5):331–338
- Shishesaz M, Shariati M, Yaghoobian A, Alizadeh A (2019) Nonlinear Vibration Analysis of Nano-Disks Based on Nonlocal Elasticity Theory Using Homotopy Perturbation Method. *Int J Appl Mech* 11(2):1950011
- Wang YZ (2017) Nonlinear internal resonance of double-walled nanobeams under parametric excitation by nonlocal continuum theory. *Appl Math Model* 48:621–634
- Yayli MO (2014) A compact analytical method for vibration analysis of single-walled carbon nanotubes with restrained boundary conditions. *J Vib Control* 22(10):2542–2555. <https://doi.org/10.1177/1077546314549203>
- Zhang L, Guo J, Xing Y (2019) Nonlocal analytical solution of functionally graded multilayered one-dimensional hexagonal piezoelectric quasicrystal nanoplates. *Acta Mech* 230:1781–1810
- Zhang L, Li X, Fang J, Long Z (2017) Multi-objective optimization of flexure hinge mechanism considering thermal–mechanical coupling deformation and natural frequency. *Adv Mech Eng* 9(1):1–17

Publisher's Note Springer Nature remains neutral with regard to jurisdictional claims in published maps and institutional affiliations.